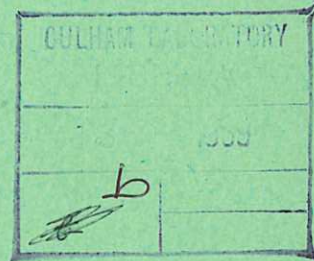
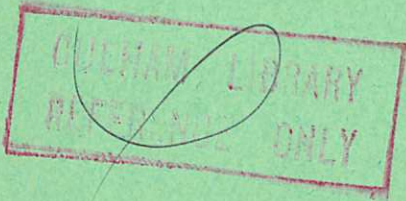


This document is intended for publication in a journal, and is made available on the understanding that extracts or references will not be published prior to publication of the original, without the consent of the author.

CLM-P212



✓

United Kingdom Atomic Energy Authority  
RESEARCH GROUP

Preprint

# A HIGH CURRENT 60 kV MULTIPLE ARC SPARK GAP SWITCH OF 1.7 nH INDUCTANCE

T. E. JAMES

Culham Laboratory  
Abingdon Berkshire

1969

Enquiries about copyright and reproduction should be addressed to the Librarian, UKAEA, Culham Laboratory, Abingdon, Berkshire, England

A HIGH CURRENT 60 kV MULTIPLE ARC SPARK  
GAP SWITCH OF 1.7 nH INDUCTANCE

by

T.E. JAMES

(To be submitted for publication in the Proceedings of the  
Institution of Electrical Engineers)

A B S T R A C T

The necessary conditions for obtaining consistent multiple arc breakdowns in a 60 kV pressurised air spark gap of 1.7 nH effective inductance have been investigated. Theoretical conclusions which are confirmed by the experimental results, show that the important factors influencing multiple arc breakdown are the gap voltage decay time and the ratio of initial arc channel impedance to that of the complete gap. The spark gap has also been used with a single 15 kJ capacitor at a peak current of 1.0 MA the combined inductance of the unit being 14 nH.

U.K.A.E.A. Research Group,  
Culham Laboratory,  
Abingdon,  
Berks.

July, 1969 (MEJ)

## C O N T E N T S

	<u>Page</u>
1. INTRODUCTION	1
2. EXPERIMENTAL APPARATUS	2
3. THEORETICAL PRINCIPLES	4
4. EXPERIMENTAL RESULTS	7
5. DISCUSSION OF RESULTS	9
6. CONCLUSIONS	11
7. ACKNOWLEDGEMENTS	12
8. REFERENCES	13

MEMORANDUM

TO : SAC, [illegible]

FROM : [illegible]

SUBJECT: [illegible]

[illegible]

[illegible]

[illegible]

[illegible]

[illegible]

[illegible]

[illegible]

[illegible]

[illegible]

[illegible]

[illegible]

[illegible]

[illegible]

[illegible]

[illegible]

[illegible]

[illegible]

[illegible]

[illegible]

---

## LIST OF SYMBOLS

$C_b$	Main capacitor
$C_t$	Trigger circuit blocking capacitor
$G_t$	Trigger circuit auxiliary gap (diversion gap only)
$L_b$	Inductance of gap connections
$L_c$	Load coil inductance
$L_d$	Effective gap inductance during voltage decay
$L_e$	Inductance of all arc channels in parallel
$L_g$	Gap inductance at high currents
$p_b$	Static breakdown pressure
$p_w$	Operating pressure
$R_1 R_2$	Resistive voltage divider
$R_t$	Trigger circuit isolation resistors
$S_1$	Multiple arc start gap
$S_2$	Multiple arc diversion gap
$\Delta t_b$	Total spread in breakdown time between points
$T_b$	Transit time of capacitor transmission line
$T_c$	Transit time of coil transmission line
$T_g$	Transit time of gap transmission line
$\tau_d$	Gap voltage decay time constant
$V_b$	Main capacitor voltage
$V_e$	Voltage between main electrodes (Fig.2b)
$V_g$	Total gap voltage (Fig.2b)
$V_t$	Intermediate electrode potential
$x$	Length of long gap spacing
$y$	Length of short gap spacing
$Z_b$	Capacitor transmission line impedance
$Z_c$	Coil transmission line impedance
$Z_g$	Gap transmission line impedance
$Z_o$	Long transmission line impedance
$Z_t$	Trigger cable impedance

## 1. INTRODUCTION

Low inductance capacitor banks for producing high current pulses of about 1.0 MA rising in a few microseconds are usually switched by numbers of single arc spark gaps connected in parallel<sup>(1,3)</sup> or by high performance solid dielectric switches<sup>(4)</sup>. The use of parallel spark gaps has proved necessary because it is difficult to reduce the inductance of such gaps much below 20 nH each whereas the complete switching system inductance may have to be as low as 1 or 2 nH. The minimum inductance that can be achieved with a single arc gap is limited to that associated with the magnetic field round the arc channel provided the connections to the electrodes are correctly designed. It follows that a significant reduction in inductance can be achieved by establishing a number of arc channels between the gap electrodes. This also enables the peak current and coulomb rating of the gap to be increased.

It has been shown that with three-electrode single arc gaps having a 'field distortion' electrode geometry as in Fig.1 small variations or 'jitter' in breakdown time of about  $\pm 2$  ns can be achieved combined with a wide operating voltage range<sup>(3)</sup>. Since these are also the conditions required for consistently producing multiple arc breakdowns this electrode geometry was also used for the multiple arc gap. The latter was developed to short circuit a 43 nH coil after one half-cycle of current (peak value 500 kA), an effective gap inductance of 1.7 nH being required for this duty. It was also used as part of a compact 36 kV, 15 kJ capacitor/spark gap unit of 14 nH combined inductance of which the gap contributed 5 nH. This unit was operated at up to a peak current of 1.0 MA. The short circuiting gap is referred to as a 'diversion' gap and that associated with the

capacitor unit as a 'start' gap. Initial triggering experiments were carried out in a low energy 60 kV circuit to study the reliability and mechanism of breakdown.

## 2. EXPERIMENTAL APPARATUS

### 2.1 Multiple Arc Gap Assembly

The two 'heavy alloy' (tungsten, copper nickel) main electrodes (A and C in Fig.1) are 2 cm diameter and 50 cm long and are bolted to aluminium alloy plates insulated by polythene sheets of 5 mm thickness. Six wedge-shaped trigger electrodes (B in Fig.1) are placed asymmetrically between the main electrodes and mounted off 2 cm diameter steel bolts. The switch plates and epoxy resin end-covers which support the trigger bolt assembly form an enclosure which can be pressurised at up to 7.0 atm absolute with dry air ( $-50^{\circ}\text{C}$  dewpoint). All electrodes and insulation details are easily replaceable to facilitate maintenance.

The trigger electrodes are initially held at an intermediate potential to give an almost uniform field distribution. A 100 kV negative voltage pulse rising at about 4 kV/ns is applied to each trigger electrode to initiate breakdown by field emission from the highly stressed edge of the electrode<sup>(3,5)</sup>. The field configuration in Fig.1 is applicable to conditions at which breakdown of the long gap occurs.

### 2.2 Capacitor/Spark Gap Assembly

The experimental arrangement of capacitor  $C_b$ , start gap  $S_1$ , diversion gap  $S_2$  and load coil  $L_c$  is as shown in Fig.2a. The 22.0  $\mu\text{F}$  capacitor has an 85 x 34 x 33 cm rectangular metal case, the transmission line BD being connected to both its long sides.



The H.T. connections A are made to a number of studs placed along the centre of the insulating lid. The rating of this unit has not yet been finally evaluated but it is anticipated that operation at 15 kJ, 36 kV, 30% voltage reversal will be possible with a reasonable life. The present experiments have been carried out at up to 30 kV, 10 kJ, 85% voltage reversal and a peak current of 1.0 MA. Similar units have been used previously in a 1.0 MJ application and have been tested at up to a peak short-circuit current of 1.2 MA<sup>(6)</sup>.

It will be shown below that the design of the terminations of all components must be such that their 'lumped' inductance (i.e. inductance without any associated capacity) is negligible compared with that of the multiple arc gap. For this reason parallel-plate geometry is adopted throughout the whole system, the diversion gap electrode plates forming part of the capacitor to load coil transmission line whose impedance  $Z_g$  is 1.0 ohm approximately. A simplified equivalent circuit can now be drawn as in Fig.2b. The inductance of gaps  $S_1$  and  $S_2$  can be divided into parts  $L_b$  and  $L_e$ . The former is the lumped inductance due to flux linking the total current and  $L_e$  is the inductance of all the arcs in parallel due to flux linking the current in each arc only. In the case of  $S_2$  it will be noted that the effective gap inductance in parallel with  $L_c$  is only  $L_e$  which can be as low as 33% of the total gap inductance. It is essential that this inductance be less than say 10% of the coil inductance if an adequate reduction in coil current is to be achieved following the closing of  $S_2$ .

### 2.3. Trigger Circuits

The triggering circuits used are as in Fig.3. In Fig.3a the trigger electrodes are electrically isolated from each other by the

resistors  $R_t$  of  $100 \Omega$ , whereas in Fig.3b they are connected in parallel by a 5 cm wide plate placed on the surface of the epoxy covers both above and below the gap.

The single trigger cable  $Z_t$ , 12 m long is initially charged to a voltage of + 60 kV, and then short circuited by a master gap across its other end. A negative voltage pulse is then produced at the trigger electrodes rising exponentially to a theoretical value of 120 kV with a time constant of about  $30 \text{ ns}^{(3)}$ . The trigger electrode is positioned so that the air gaps  $x$  and  $y$  in Fig.3a are in the ratio 70:30, the larger gap being towards the positive H.T. electrode (Figs.1 and 3) so that it breaks down first. The total air gap ( $x + y$ ) is 7 and 5 mm for 60 kV and 30 kV working respectively.

The trigger system used for the diversion gap is shown in Fig.3b with the auxiliary gap  $G_t$  in circuit. The latter is necessary to isolate the trigger cable during the first half cycle of voltage 'hold-off' to enable the resistive divider  $R_1R_2$  to control accurately the potential of the trigger electrodes. It is arranged that  $G_t$  breaks down near the maximum value of the trigger pulse so that the pulse applied to the trigger electrodes is 'steepened'<sup>(3)</sup>.

The decay of gap voltage was measured with a resistive voltage divider and fast rise oscilloscope with a combined response time of 2.5 ns. Satisfactory multiple arc triggering was diagnosed by placing a magnetic probe near each breakdown point as reported previously<sup>(7)</sup>. Using this technique, if a point failed to break down the measured magnetic field was reduced to less than a third of its normal value.

### 3. THEORETICAL PRINCIPLES

To achieve multiple arc breakdowns between a single pair of electrodes their spread in breakdown time  $\Delta t_p$  must be less than the

decay of the electrode voltage  $V_e$  (Fig.4) to the minimum value at which complete breakdown can occur. The problem is similar to that encountered when parallel single arc gaps are used without any transit time isolation between them. The latter have been operated successfully using the field distortion geometry in Fig.3, and also using trigatron gaps<sup>(8)</sup>. In the latter case the importance of the gap voltage decay time was demonstrated by varying the capacity in parallel with the gaps. However, the successful achievement of multiple arc breakdowns is more difficult than the parallel operation of single arc gaps because of the decay of electrode voltage  $V_e$  due to early breakdowns. The voltage decay is accelerated by the inductive division  $L_e/(L_b + L_e)$  of the gap voltage  $V_g$ , which is itself decaying with a time constant  $\tau_d$  equal to  $(L_b + L_e)/Z_g$ . This inductance ratio must therefore be kept high by choosing the gap geometry so that  $L_b$  is minimised.

$L_e$  is an effective arc inductance which for convenience includes the effect of the arc resistive voltage drop, since the approximately exponential decay of the latter means that the resistive and inductive voltages have similar characteristics. The effective gap inductance  $L_d$  which applies during the decay of gap voltage equals  $(L_b + L_e)$  and is deduced from measurements of the gap voltage decay time  $\tau_d$  since this equals  $L_d/Z_g$ .

To ensure that the gap voltage time  $\tau_d$  is adequate the gap should be connected into a transmission line of sufficiently low impedance  $Z_g$  and having a sufficiently long transit time  $T_g$  of say, 5 to 10 ns. These requirements are satisfied by the assembly shown in Fig.2a.

Following the application of the negative trigger voltage pulse

to each of the six trigger electrodes, their potential  $V_t$  (i.e. the voltage across gap  $y$  in Fig.3b) will be as curve ABC in Fig.4 for the first breakdown point and as curve ADE for the last breakdown point. The difference between these two curves has been exaggerated to simplify the diagram. The large gap spacings ( $x$  in Fig.3a) break down at B and D and the smaller spacing at C for the first point. After the complete breakdown of the first point at C, the electrode voltage  $V_e$  will decay with the time constant  $\tau_d = L_d/Z_g$ , which will depend on the circuit parameters as discussed above and the time distribution of the breakdown of later points. For the last point to break down completely its smaller spacings ( $x$  in Fig.3) would have to be sufficiently overstressed by the voltage EG when  $V_e$  has fallen to F. This is most likely to be achieved with asymmetrically placed trigger electrodes, and a trigger circuit design such that the overshoot in trigger electrode potential (EF in Fig.4) is a maximum. Both these aspects have been studied in detail during the development of single arc gaps<sup>(1,2,3)</sup>.

The above discussion assumes that both gap spacings at a given point break down in 'cascade'. However, over a small voltage range of about 5 to 10% of the maximum working voltage, it is possible to arrange that at a given pressure the trigger pulse breaks down both gap spacings (e.g. at point B in Fig.4) before the 'swing' in the trigger electrode potential back to  $V_e$  occurs. This mode of operation is referred to as 'simultaneous' breakdown<sup>(3)</sup>. It has the advantage that the breakdown time and jitter are minimised but since the electrode spacings and trigger circuit parameters need more careful optimisation operation in the cascade mode is considered to be easier to achieve.

#### 4. EXPERIMENTAL RESULTS

##### 4.1 Effect of Transmission Line Impedance

The first experiments were carried out with a 4 m long line, placed between the start gap and a 60 kV capacitor as reported previously<sup>(7)</sup>, the impedance  $z_0$  of the line being varied from 0.5 to 4.0 ohms. This arrangement ensured that the gap was connected to a fixed impedance for 40 ns, a time long compared with its breakdown time. The trigger circuit used was as in Fig.3(a).

The number of breakdowns that occur as a function of the number of triggered points and  $z_0$  are given in Fig.5. Each point represents the mean of 20 shots, i.e. 120 triggered points when six points are triggered. The decay time of the gap voltage  $V_d$  deduced from these results and hence the gap inductance  $L_d$  during this time are given in Fig.6. With six triggered points the variation in breakdown time was  $\pm 1.0$  ns. The gap voltage ( $V_g$ ) waveforms and magnetic probe measurements for the various conditions have already been reported<sup>(7)</sup>.

##### 4.2 Variation of Trigger Circuits

The above experiments were repeated both with the 'separate' trigger circuits in Fig.3a, and the 'common' trigger circuits in Fig.3b, the line impedance being  $0.5\Omega$  in each case. The absolute operating air pressure in the gap  $p_w$  was varied from 4.0 to 7.0 atm, the static breakdown pressure being 3.3 atm. The number of breakdowns with six triggered points is given in Fig.7.

##### 4.3 High Current Tests With 22.0 $\mu$ F Capacitor

The gap was assembled in position  $S_1$  as in Fig.2a. The combined inductance of the capacitor, spark gap and connections was obtained by connecting the upper transmission line D to the middle transmission line BC. With six triggered points at 25 kV, and a peak

current of 0.9 MA resonant frequency was 281 kHz with 85% reversal giving a combined inductance and resistance of 14.3 nH and 2.6 m $\Omega$  respectively. The variation in gap inductance  $L_g$  with the number of triggered points as given in Fig.8 was deduced by measuring the change in frequency of a similar capacitor/spark gap assembly (about 300 kA peak current) and subtracting the measured capacitor inductance. The total gap inductance with six triggered points is  $5 \text{ nH} \pm 1.0 \text{ nH}$ .

The capacitor inductance was measured by placing an 0.1 mm insulation sheet between transmission lines B and A with a small hole placed in its centre which breaks down at about 3 kV. The resulting current waveform was not perfectly sinusoidal but its average frequency was 435 kHz giving an inductance of 6.0 nH.

High current short-circuit tests were made at 30 kV, 1.0 MA for a few hundred shots with the transmission lines short circuited at DC. Further tests were made with the single turn coil  $L_c$  of 43 nH connected to DC. The number of breakdowns in the start gap  $S_1$  using the common trigger circuit (Fig.3b) and with six triggered points was again noted with and without  $L_c$  and in both cases was found to be comparable with those obtained with the 4 m line in Fig.7.

#### 4.4 Diversion Gap Performance

The diversion gap  $S_2$  (Fig.2) was operated with the common trigger system (Fig.3b) and six triggered points to short circuit the 43 nH load coil after one half cycle of current. The capacitor voltage  $V_b$  was + 30 kV and the peak coil current 500 kA rising in 2  $\mu$ s. The coil and capacitor currents are given in Fig.9a and b for eight consecutive shots showing that the former is consistently reduced to less than 5% of its peak value by the diversion gap. The

effective gap inductance  $L_e$  (Fig.2) in this duty as deduced from analysis of the waveforms in Fig.9 is  $1.7 \text{ nH} \pm 0.2 \text{ nH}$ .

## 5. DISCUSSION OF RESULTS

### 5.1 Number of Multiple Arc Breakdowns

The results in Figs.5 and 6 show that as the gap voltage decay time decreases it becomes more difficult to achieve a higher proportion of breakdowns as would be expected from the discussion in Section 3. Under these triggering conditions for all triggered points to break down the voltage decay time constant should be at least 20 ns. A comparison of the triggering performance with separate and common trigger circuits in Fig.7 shows that in the latter case a small improvement in the number of breakdowns occurs. It is considered that this is because the close connection of the trigger electrodes probably delays the swing in potential of the early intermediate electrodes to break down and consequently delays the completion of breakdown at these points and also the onset of the decay of gap voltage. This would then reduce the spread in breakdown time between the various points and therefore make it easier for multiple breakdowns to be achieved.

As the operating pressure  $p_w$  is increased from near the static breakdown value  $p_b$  to about twice  $p_b$  a small but significant improvement in the number of breakdowns occurs with both trigger circuits as shown in Fig.7. This result is rather surprising since it would normally be expected that when operating in the cascade mode the breakdown time and jitter would increase as the pressure is increased until conditions that will result in simultaneous breakdown are reached. Previous measurements of formative breakdown times in similar non-uniform field single arc gaps<sup>(3,5)</sup> indicate that in the

present gap simultaneous breakdown would occur with a value of  $p_w/p_b$  of about 2.0 which is the pressure at which the best performance is achieved in Fig.7. This therefore suggests that this improved performance is due to operation in the simultaneous mode and that this is more easily achieved with closely connected intermediate electrodes as in Fig.3b. Under these conditions 98% of the triggered points break down in 20 consecutive shots.

## 5.2 Gap Parameters

Immediately after breakdown the gap impedance, as represented by the values of effective inductance  $L_d$  given in Fig.6, increases appreciably as the line impedance increases from 0.5 to 4.0 ohms for a given number of breakdown points. This is mainly caused by the effect of the differing rates of rise of current on the resistive component of the arc voltage. It results in a non-linear dependence of the voltage decay time constant  $\tau_d$  on  $Z_0$ . In these experiments  $\tau_d$  varies as  $Z_0^{-1/2}$  approximately, but this will only apply in general to gaps of similar inductance.

The gap inductance  $L_g$  obtained at high currents as given in Fig.8, decreases only by about 10% as the number of breakdown points increase from four to six, so that provided more than, say, 80% of the points break down the total gap inductance will be about 5 nH. The value of the various inductances given in the equivalent circuit (Fig.2b) during the voltage decay time and at high currents can now be summarised as in Table I for six breakdown points with the gap connected to an equivalent 1 ohm line.



TABLE I

Values of Gap and Arc Channel Inductance

	During voltage decay	At high currents
Arc Channels ( $L_e$ )	11.7* nH	1.7 nH
Gap connections ( $L_b$ )	3.3	3.3
Total inductance	15* (= $L_d$ )	5 (= $L_g$ )
	*Effective values	

It should be noted in Table I that the initial ratio of  $L_e/L_d$  (and therefore  $V_e/V_g$ ) is about 0.8 and so the rapid decay of the electrode voltage that would be produced by inductive division is limited to 20%. The important factors in this respect are the high initial impedance of the arc channels (about seven times the final value) and the low value achieved for the common inductance  $L_b$  by careful design of the gap connections.

## 6. CONCLUSIONS

The initiation of multiple arc breakdown between the electrodes of the 60 kV pressurised air spark gap described has been consistently achieved. The experimental results confirm that the important factors influencing multiple arc breakdown are an adequate gap voltage decay time (say 15 to 20 ns), a small spread in breakdown time between the breakdown points and a high ratio of effective arc inductance to total gap inductance. When assembled as a compact unit with a 15 kJ 36 kV capacitor operating at up to a peak current of 1.0 MA the combined inductance is 14 nH of which the gap contributes 5 nH. The effective gap inductance can be reduced to 1.7 nH, when it is used to short circuit a low inductance load coil, by mounting the gap in the capacitor to load coil transmission line.

## 7. ACKNOWLEDGEMENTS

The author wishes to acknowledge helpful discussions with Mr. J.C. Martin, A.W.R.E, Aldermaston, on the principles of multiple arc spark gaps, and with the design staff of BICC, Capacitor Division, Helsby, who developed the low inductance capacitors.

The preliminary experimental work<sup>(7)</sup> was carried out by Mr. J.E. Gruber and Mr. F.J. Kivlin, and Dr. H. Enjoji assisted with the development of the final trigger system. Mr. K. Harries and Mr. G.D. Harding were responsible for mechanical design and manufacture and Mr. J. Talboys for the installation and operation of the experimental equipment.

## 8. REFERENCES

1. FITCH, R.A. and McCORMICK, N.R.: 'Low inductance switching using parallel spark gaps', Proc. I.E.E., 1959, 106A, Suppl.2, pp.117-130
2. FITCH, R.A. and McCORMICK, N.R.: 'The modes of operation of a cascade spark gap for precision switching', 4th Int. Conf. on Ionized Gases, Uppsala, 1959, Proc. Vol.1, (Amsterdam, 1960) pp.463-7
3. BARNES, P.M., GRUBER, J.E. and JAMES, T.E.: 'The parallel operation of low inductance high current spark gaps, without transit time isolation', J. Sci. Instrum., 1967, 44, pp.599-605
4. BARNES, P.M., HARRIES, K., JAMES, T.E. and PHILLPOTT, J.: 'A multiple arc, 100 kV, 2.0 MA solid dielectric switch'. To be published.
5. GRUBER, J.E. and JAMES, T.E.: 'Fast pulse breakdown of non-uniform field pressurised air spark gaps'. Proc. I.E.E., 1968, 115, pp.1530-1534
6. MARTIN, J.C. and MACAULEY, A.: 'A cheap megajoule bank'. Symposium on Fusion Technology, Oxford 1968, Paper No.33, A.W.R.E. Aldermaston report
7. JAMES, T.E., GRUBER, J.E. and KIVLIN, F.J.: 'The initiation of multiple arc breakdowns in a 60 kV low inductance spark gap'. 8th Int. Conf. on Ionized Gases, Vienna, 1967, Contributed Papers (Springer-Verlag, 1968), p.203

8. FRIEDRICH, F.J. and HINTZ, E.: 'The simultaneous switching of many parallel trigatrons without decoupling leads'. Proc. of Symposium on Problems of C.T.R.', Gatlinburg, U.S.A. October 1966, Oak Ridge National Laboratory, Conf. 661016, p.3

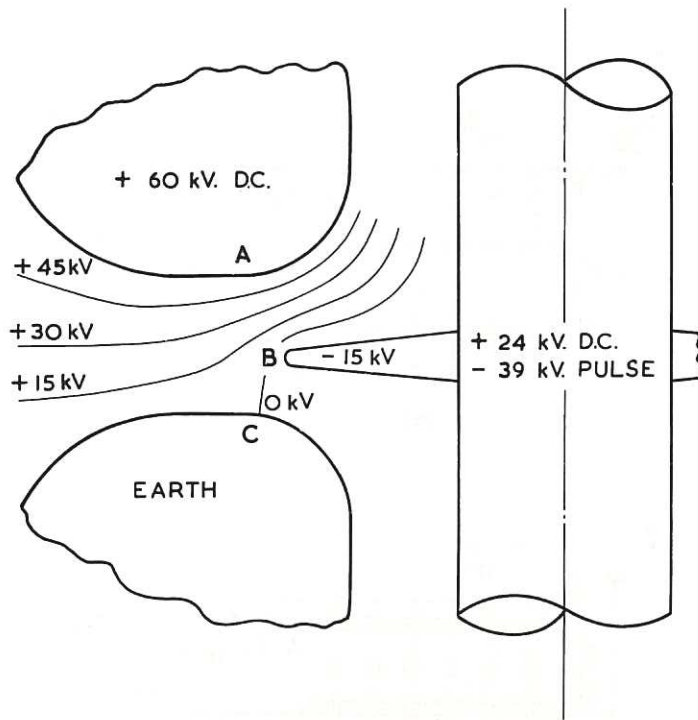


Fig.1 'Field distortion' electrode geometry and field configuration

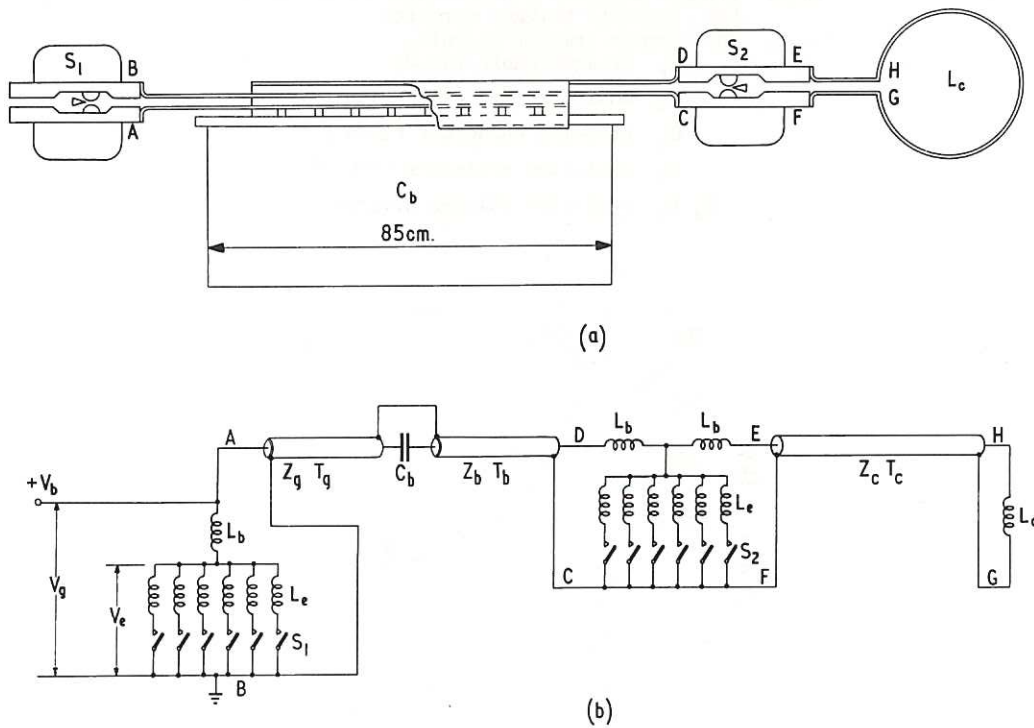


Fig.2 Multiple arc gap and capacitor assembly

(a) General arrangement

(b) Equivalent circuit

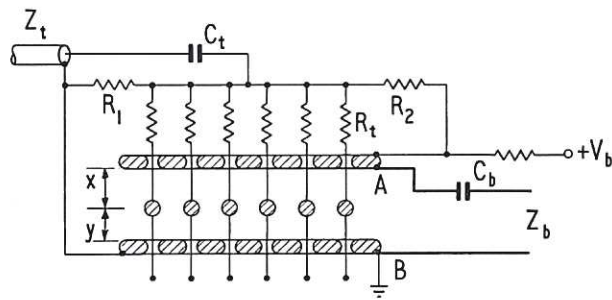
$C_b$  capacitor

$S_1$  start gap

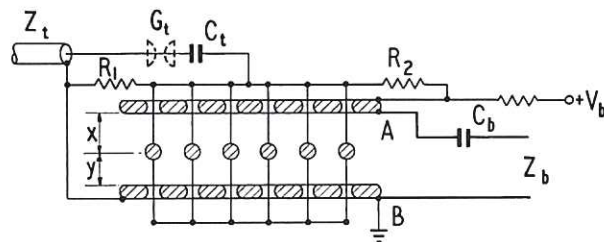
$S_2$  diversion gap

$L_c$  load coil

CLM-P212



(a)



(b)

Fig.3 Trigger circuits and electrode arrangement

(a) Separate trigger circuits

(b) Common trigger circuits

$Z_t$  trigger cable (50  $\Omega$ )

$G_t$  auxiliary gap (diversion duty only)

$C_t$  blocking capacitor (2000 pF)

$R_t$  isolation resistors (100  $\Omega$ )

$R_1$   $R_2$  resistive voltage divider

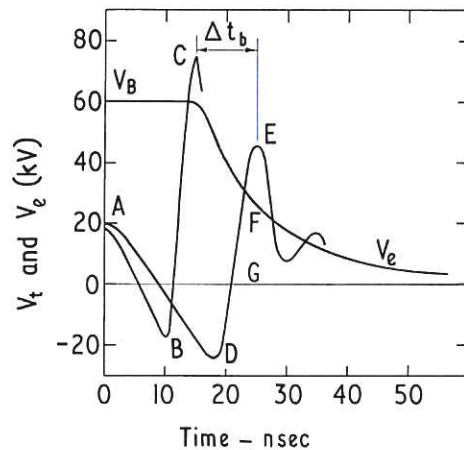


Fig.4 Typical main electrode voltage ( $V_e$ ) and trigger electrode potential ( $V_t$ ) curves after the application of the trigger voltage pulse at point A. Curve ABC for first breakdown points ( $V_t$ ) Curve ADE for last breakdown point ( $V_t$ )

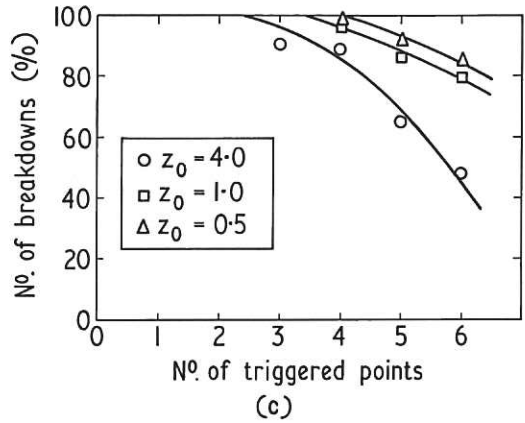


Fig.5 The number of breakdowns as a function of transmission line impedance and number of triggered points for separate trigger circuits  
 $V_b = + 60 \text{ kV}$   $p_w = 5.0 \text{ atm}$

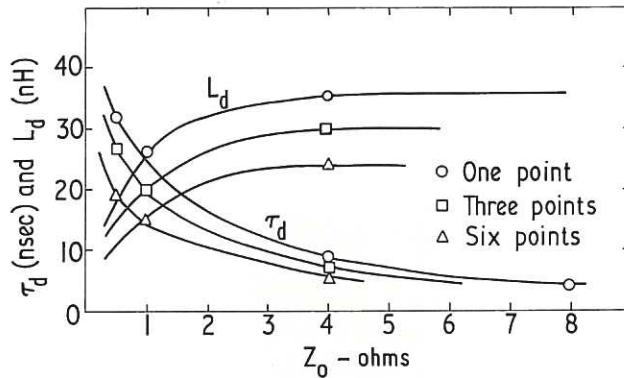


Fig.6 The decay time constant ( $\tau_d$ ) of the gap voltage  $V_g$ , and the initial effective gap inductance ( $L_d$ ), as a function of the transmission line impedance ( $Z_0$ ) and the number of breakdown points  
 $V_b = + 60 \text{ kV}$   $p_w = 5.0 \text{ atm}$

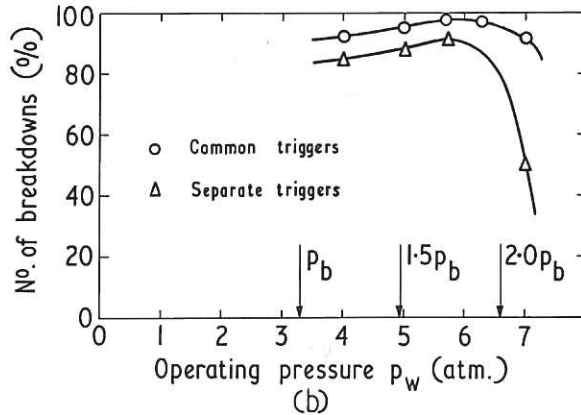


Fig.7 The effect of different trigger circuits on the number of breakdowns at various operating pressures ( $p_w$ )  
 $Z_0 = 0.5 \Omega$   
 $V_b = + 60 \text{ kV}$   
 6 triggered points

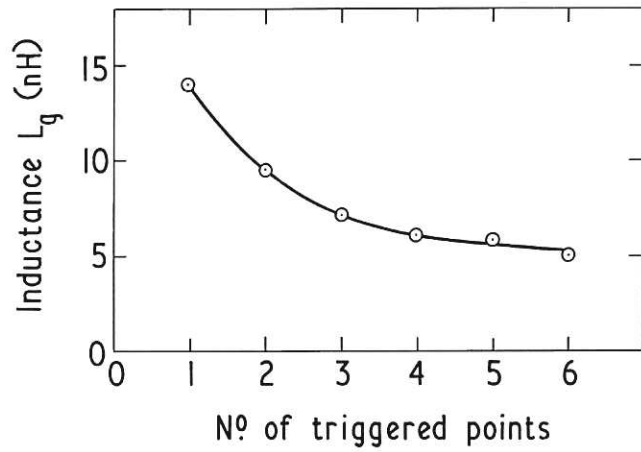
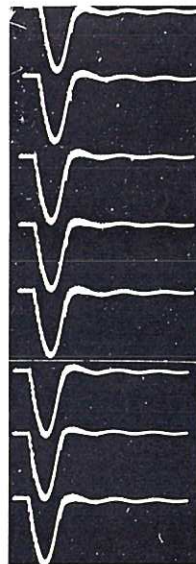
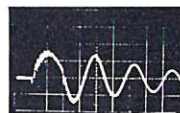


Fig.8 The gap inductance  $L_g$  as a function of the number of breakdown points  
 Peak current 300 kA  
 Circuit frequency 900 kHz



(a)



(b)

Fig.9 Diverted circuit current waveforms  
 (a) Load coil current  
 (b) Capacitor current ( $2\mu\text{s}/\text{div}$ ) CLM-P212





